articles

molecular pharmaceutics

Shrinkage of a Rapidly Growing Tumor by Drug-Loaded Polymersomes: pH-Triggered Release through Copolymer Degradation

Fariyal Ahmed,[†] Refika I. Pakunlu,[‡] Goundla Srinivas,[§] Aaron Brannan,[||] Frank Bates,[||] Michael L. Klein,[§] Tamara Minko,[‡] and Dennis E. Discher*,[†]

Chemical and Biomolecular Engineering, University of Pennsylvania, Philadelphia, Pennsylvania 19104, Center for Molecular Modeling, Department of Chemistry, University of Pennsylvania, Philadelphia, Pennsylvania 19104, Pharmaceutics, Rutgers, The State University of New Jersey, Piscataway, New Jersey 08854, and Chemical Engineering & Material Science, University of Minnesota, Minneapolis, Minnesota 55455

Received November 12, 2005

Abstract: Carrier-mediated delivery of drugs into the cytosol is often limited by either release from the carrier or release from an internalizing endolysosome. Here, loading, delivery, and cytosolic uptake of drug mixtures from degradable polymersomes are shown to exploit both the thick membrane of these block copolymer vesicles and their aqueous lumen as well as pH-triggered release within endolysosomes. Our initial in vivo studies demonstrate growth arrest and shrinkage of rapidly growing tumors after a single intravenous injection of polymersomes composed of poly(ethylene glycol)−polyester. Vesicles are shown to break down into membranelytic micelles within hours at 37 °C and low pH, although storage at 4 °C allows retention of drug for over a month. It is then shown that cell entry of the polymersomes into endolysosomes is followed by copolymer-induced endolysosomal rupture with release of cytotoxic drugs. Above a critical poration concentration (C_{CPC}) that is easily achieved within endolysosomes and that scales with copolymer proportions and molecular weight, the copolymer micelles are seen to disrupt lipid membranes and thereby enhance drug activity. Neutral polymersomes and related macrosurfactant assemblies can thus create novel pathways within cells for controlled release and delivery.

Keywords: Drug delivery; polymer vesicles; cancer chemotherapy; PEG-PLA

Introduction

Some polymeric carrier systems, such as cationic polymers used to condense DNA, can create their own intracellular pathways for delivery of therapeutics and dyes. Cationic polymers mediate endosomal rupture through a "proton sponge" effect.[1−3] However, positive charge in vivo leads to clearance within minutes from the circulation,[4] a problem that has motivated efforts (often unsuccessful) to shield charge with neutral polymers such as poly(ethylene glycol)

* Corresponding author. Mailing address: Chemical and Biomolecular Engineering, Graduate Groups in Physics, Cell & Molecular Biology, University of Pennsylvania, 112 Towne Bldg., Philadelphia, PA 19104-6393. Tel: (215) 898-4809. Fax: (215) 573-6334. E-mail address: discher@seas.upenn.edu.

[†] Chemical and Biomolecular Engineering, University of Pennsylvania.

[‡] Rutgers, The State University of New Jersey.

[§] Center for Molecular Modeling, Department of Chemistry, University of Pennsylvania.

[||] University of Minnesota.

(1) Sonawane, N. D.; Szoka, F. C.; Verkman, A. S. Chloride accumulation and swelling in endosomes enhances DNA transfer by polyamine-DNA polyplexes. *J. Biol. Chem.* **2003**, *278*, 44826−44831.

(2) Lim, Y.-B.; Kim, S.-M.; Suh, H.; Park, J.-S. Biodegradable, endosome disruptive, and cationic network-type polymer as a highly efficient and nontoxic gene delivery carrier. *Bioconjugate Chem.* **2002**, *13*, 952−957.

10.1021/mp050103u CCC: $33.50
Published on Web 03/18/2006

Table 1. Properties of Amphiphilic A-B Diblock Copolymers Studied

copolymer name	formula A_m-B_n	M_n (kg/mol)	PD	f_{EO}	core thickness, d (nm)
OCL1	EO_{46}-CL_{24}	4.8	1.19	0.42	9.3
OL2	EO_{109}-LA_{56}	10.0	1.16	0.49	11.4
OB18	EO_{80}-BD_{125}	10.4	1.10	0.29	14.8

(PEG).[5] Block copolymer vesicles made from PEG-based amphiphiles[6−13] directly integrate such a brush into every molecule. As a result, these neutral vesicles or "polymersomes" avoid rapid clearance by the liver and spleen and can thus circulate intact for more than a day in rats.[14] This now motivates the design of polymer-based mechanisms for drug entry into cells, or more specifically drug entry into cell cytoplasm. Here we illustrate how drug-loaded polymersomes based on PEG-(polylactic acid, PLA) and PEG-(polycaprolactone, PCL) (Table 1) not only carry diverse anticancer agents but will also enter cells, facilitate delivery to subcellular targets, and shrink tumors.

The drug-loaded polymersomes described here exploit the combination of a thick wall for a hydrophobic drug such as paclitaxel (TAX) and a vesicular lumen for a hydrophilic drug such as doxorubicin (DOX). Recent clinical studies show that cocktails of water-insoluble TAX with water-soluble DOX lead to better tumor regression compared to either drug alone,[15] but carriers for both of these drugs can better ensure simultaneous delivery to each cell while extending drug circulation times and limiting off-target toxicity. TAX loaded into liposome membranes reduces both the toxicity typical of TAX emulsions[16] and TAX's neurotoxicity,[17] but high concentrations of TAX destabilize thin lipid membranes.[18] This has motivated the development of copolymer micelles with cores tailored to hydrophobic drugs.[19,20] Likewise, liposomal DOX and polymer-based DOX carriers limit rapid excretion of free drug[21−23] as well as cardiotoxicity,[24] but liposomes often prove leaky and lipid PEG-ylation limits drug release at the tumor.[25] Controlled release polymersomes[13] with thick membranes[6,12] for TAX loading as well as aqueous interiors for DOX loading address the above issues of long circulation and release, and perhaps most interesting they also provide intrinsic mechanisms for endosomal escape.

(3) Putnam, D.; Gentry, C. A.; Pack, D. W.; Langer, R. Polymer-based gene delivery with low cytotoxicity by a unique balance of side-chain termini. *Proc. Natl. Acad. Sci. U.S.A.* **2001**, *98*, 1200−1205.

(4) Barron, L. G.; Gagne, L.; Szoka, F. C. Lipoplex-mediated gene delivery to the lung occurs within 60 minutes of intravenous administration. *Hum. Gene Ther*. **1999**, *10*, 1683−1694.

(5) Klibanov, A. L.; Maruyama, K.; Torchilin, V. P.; Huang, L. Amphipathic polyethyleneglycols effectively prolong the circulation time of liposomes. *FEBS Lett.* **1990**, *268*, 235−237.

(6) Discher, D. E.; Eisenberg, A. Polymer vesicles. *Science*. **2002**, *297*, 967−973.

(7) Graff, A.; Sauer, M.; Van Gelder, P.; Meier, W. Virus-assisted loading of polymer nanocontainer. *Proc. Natl. Acad. Sci. U.S.A.* **2002**, *99*, 5064−5068.

(8) Savic, R.; Luo, L.; Eisenberg, A.; Maysinger, D. Micellar nanocontainers distribute to defined cytoplasmic organelles. *Science* **2003**, *300*, 615−618.

(9) Napoli, A.; Valentini, M.; Tirelli, N.; Muller, M.; Hubbell, J. A. Oxidation-responsive polymeric vesicles. *Nat Mater*. **2004**, *3*, 183−189.

(10) Haining, W. N.; Anderson, D. G.; Little, S. R.; von Berwelt-Baildon, M. S.; Cardoso, A. A.; Alves, P.; Kosmatopoulos, K.; Nadler, L. M.; Langer, R.; Kohane, D. S. pH-Triggered Microparticles for Peptide Vaccination. *J. Immunol*. **2004**, *173*, 2578−2585.

(11) Lee, M.; Lee, S.-J.; Jiang, L.-H. Stimuli-Responsive Supramolecular Nanocapsules from Amphiphilic Calixarene Assembly. *J. Am. Chem. Soc*. **2004**, *126*, 12724−12725.

(12) Discher, B. M.; Won, Y. Y.; Ege, D. S.; Lee, J. C. M.; Bates, F. S.; Discher, D. E.; Hammer, D. A. Polymersomes: tough vesicles made from diblock copolymers. *Science* **1999**, *284*, 1143−1146.

(13) Ahmed, F.; Discher, D. E. Self-porating polymersomes of PEG-PLA and PEG-PCL: hydrolysis-triggered controlled release vesicles. *J. Controlled Release* **2004**, *96*, 37−53.

(14) Photos, J. P.; Bacakova, L.; Discher, B.; Bates, F. S.; Discher, D. E. Polymer vesicles in vivo: correlations with PEG molecular weight. *J. Controlled Release* **2003**, *90*, 323−334.

(15) Amadori, D.; Frassineti, G. L.; Zoli, W.; Milandri, C.; Serra, P.; Tienghi, A.; Ravaioloi, A.; Gentile, A.; Salzano, E. Doxorubicin and paclitaxel (sequential combination) in the treatment of advanced breast cancer. *Oncology* **1997**, *4*, 30−33.

(16) Dorr, R. T. Pharmacology and toxicology of Cremophor EL diluent. *Ann. Pharmacother*. **1994**, *28*, 11−14.

(17) Park, J. W. Liposome-based drug delivery in breast cancer treatment. *Breast Cancer Res*. **2002**, *4*, 95−99.

(18) Immordino, M. L.; Brusa, P.; Arpicco, S.; Stella, B.; Dosio, F.; Cattel, L. Preparation, characterization, cytotoxicity and pharmacokinetics of liposomes containing docetaxel. *J. Controlled Release* **2003**, *91*, 417−429.

(19) Iijima, M.; Nagasaki, Y.; Okada, T.; Kato, M.; Kataoka, K. Core-polymerized reactive micelles from heterotelechelic amphiphilic block copolymers. *Macromolecules*. **1999**, *32*, 1140−1146.

(20) Shuai, X.; Merdan, T.; Schaper, A. K.; Xi, F.; Kissel, T. Core-cross-linked polymeric micelles as paclitaxel carriers. *Bioconjugate Chem*. **2004**, *15*, 441−448.

(21) Sengupta, S.; Eavarone, D.; Capila, I.; Zhao, G.; Watson, N.; Kiziltepe, T.; Sasisekharan, R. Temporal targeting of tumor cells and neovasculature with a nanoscale delivery system. *Nature* **2005**, *436*, 568−572.

(22) Bae, Y.; Nishiyama, N.; Fukushima, S.; Koyama, H.; Yasuhiro, M.; Kataoka, K. Preparation and Biological Characterization of Polymeric Micelle Drug Carriers with Intracellular pH-Triggered Drug Release Property: Tumor Permeation, Controlled Subcellular Drug Distribution, and Enhanced in Vivo Antitumor Efficacy. *Bioconjugate Chem*. **2005**, *16*, 122−130.

(23) Omayra, L.; Padilla, D. J.; Henrik, R. I.; Gagne, L.; Frechet, J. M. J.; Szoka, F. C. Polyester dendritic systems for drug delivery applications: in vitro and in vivo evaluation. *Bioconjugate Chem.* **2002**, *13*, 453−461.

(24) Kluza, J.; Marchetti, P.; Gallego, M.-A.; Lancel, S.; Fournier, C.; Loyens, A.; Beauvillain, J.-C.; Bailly, C. Mitochondrial proliferation during apoptosis induced by anticancer agents: effects od doxorubicin and mitoxantrone on cancer and cardiac cells. *Oncogene* **2004**, epub, 1−13.

(25) Hong, R.-L.; Huang, C.-J.; Tseng, Y.-L.; Pang, V. F.; Chen, S.-T.; Liu, J.-J.; Chang, F.-H. Direct comparison of Liposomal Doxorubicin with or without Polyethylene Glycol coating in C-26 tumor-bearing mice: Is surface coating with Polyethylene Glycol beneficial? *Clin. Cancer Res*. **1999**, *5*, 3645−3652.

Here, as initial motivation for mechanistic studies, degradable polymersomes containing high drug loads of both TAX and DOX are first shown to localize within human tumors in nude mice and shrink the tumors significantly within a day. In vitro time scales of polymersome activity appear very similar, with mechanisms based in part on copolymer-induced endolysosomal rupture due to high confinement concentrations. To help clarify copolymer lysis mechanism, coarse-grained molecular dynamics simulations show how polymeric macrosurfactants can interact with cell membranes (above a critical interaction concentration) and create pathways for cell-level therapy.

Materials and Methods

Copolymers and Chemicals. Diblock copolymers[13] are listed in Table 1. EO is ethylene oxide, M_n is number-average molecular weight, and PD is the polydispersity index. Mean hydrophobic molecular weight $M_h \approx M_n(1 - f_{EO})$, and chain lengths of the hydrophobic blocks provide a simple scaling for membrane core thickness as $d \sim (M_h)^{0.55}$.[52] TAX (± Oregon Green as a conjugate), Lysotracker Blue, Hoechst dye, fluorescein-5-carbonyl azide, and tetramethylrhodamine-5-carbonylazide (TMRCA) are from Molecular Probes (Eugene, OR). Dialysis tubing is from Spectrum Laboratories (Rancho Dominguez, CA), and dram vials are from Fisher Scientific (Suwanee, GA). The TUNEL cell death detection kit is from Roche Diagnostics (Mannheim, Germany). DOX, PKH26 red, PKH74 green, sucrose, nocodazole, genistein, chlorpromazine, ammonium chloride, chloroform, phosphate buffer (PBS), and MES buffer are all from Sigma (St. Louis, MO).

Fluorescent tagging of OL2 block copolymer with TMCRA[13] shows two fully resolved peaks on a C18 HPLC

(26) Abraham, S. A.; Edwards, K.; Karlsson, G.; MacIntosh, S.; Mayer, L. D.; McKenzie, C.; Bally, M. B. Formation of transition metal-doxorubicin complexes inside liposomes. *Biochim. Biophys. Acta* **2002**, *1565*, 41−54.

(27) Santos, N. D.; Cox, K. A.; McKenzie, C. A.; Baarda, F. v.; Gallagher, R. C.; Karlsson, G.; Edwards, K.; Mayer, L. D.; Allen, C.; Bally, M. B. pH gradient loading of anthracyclines into cholestrol-free liposomes: enhancing drug loading rates through use of ethanol. *Biochim. Biophys. Acta* **2004**, *1661*, 47−60.

(28) Grayson, A. C.; Cima, M. J.; Labnger, R. Size and temperature effects on poly(lactic-co-glycolic acid) degradation and microreservoir device performance. *Biomaterials* **2005**, *26*, 2137−2145.

(29) Ivanova, T.; Panaiotov, I.; Boury, F.; Proust, J. E.; Benoit, J. P.; Verger, R. Hydrolysis kinetics of poly(D,L-lactide)monolayers spread on basic or acidic subphases. *Colloids Surf., B* **1997**, *8*, 217−225.

(30) Belguise, K.; Kersual, N.; Galtier, F.; Chalbos, D. FRA-1 expression level regulates proliferation and invasiveness of breast cancer cells. *Oncogene* **2005**, *24*, 1434−1444.

(31) Hashizume, H.; Baluk, P.; Morikawa, S.; McLean, J. W.; Thurston, G.; Roberge, S.; Jain, R. K.; McDonald, D. M. Openings between Defective Endothelial Cells Explain Tumor Vessel Leakiness. *Am. J. Pathol*. **2000**, *156*, 1363−1380.

(32) Panyam, J.; Zhou, W.-Z.; Prabha, S.; Sahoo, S. K.; Labhasetwar, V. Rapid endo-lysosomal escape of poly(DL-lactide-co-glycolide) nanoparticles: implications for drug and gene delivery. *FASEB J*. **2002**, *16*, 1217−1226.

(33) Lee, J. C. M.; Bermudez, H.; Discher, B. M.; Sheehan, M. A.; Won, Y. Y.; Bates, F. S.; Discher, D. E. Preparation, stability, and in vitro performanceof vesicles made with diblock copolymers. *Biotechnol. Bioeng*. **2001**, *73*, 135−145.

(34) Suh, J.; Wirtz, D.; Hanes, J. Efficient active transport of gene nanocarriers to the cell nucleus. *Proc. Natl. Acad. Sci. U.S.A.* **2003**, *100*, 3878−3882.

(35) Rejman, J.; Oberle, V.; Zuhorn, I. S.; Hoekstra, D. Size-dependent internalization of particles via the pathways of clathrin-and caveolae-mediated endocytosis. *Biochem. J*. **2004**, *377*, 159−169.

(36) Qu, X.; Wan, C.; Becker, H.-C.; Zhong, D.; Zewail, A. H. The anticancer-DNA complex: Femtosecond primary dynamics for anthracycline antibiotics function. *Proc. Natl. Acad. Sci. U.S.A.* **2001**, *98*, 14212−14217.

(37) Saul, J. M.; Annapragada, A.; Natarajan, J. V.; Bellamkonda, R. V. Controlled targeting of liposomal doxorubicin via the folate receptor in vitro. *J. Controlled Release* **2003**, *92*, 49−67.

(38) Suh, J.; Dawson, M.; Hanes, J. Real-time multiple-particle tracking: applications to drug and gene delivery. *Adv. Drug Delivery Rev.* **2005**, *57*, 63−78.

(39) Lee, S. E.; Na, K.; Bae, Y. H. Super pH-Sensitive Multifunctional Polymeric Micelle. *Nano Lett.* **2005**, *5*, 325−329.

(40) Thanou, M.; Duncan, R. Polymer-protein and polymer-drug conjugates in cancer therapy. *Curr. Opin. Invest. Drugs* **2003**, *4*, 701−709.

(41) Muggia, F. M. Doxorubicin-Polymer Conjugates: Further Demonstration of the Concept of Enhanced Permeability and Retention. *Clin. Cancer Res*. **1999**, *5*, 7−8.

(42) Hubbell, J. A. Enhancing Drug Function. *Science* **2003**, *300*, 595−596.

(43) Cho, M. J.; Asokan, A. Exploitation of Intracellular pH gradients in the Cellular Delivery of Macromolecules. *J. Pharm. Sci*. **2002**, *91*, 903−913.

(44) Mellman, I.; Fuchs, R.; Helenius, A. Acidification of the Endocytic and Exocytic Pathways. *Annu. Rev. Biochem*. **1986**, *55*, 663−700.

(45) Lee, S. C.; Kim, C.; Kwon, I. C.; Chung, H.; Jeong, S. Y. Polymeric micelles of poly(2-ethyl-2-oxazoline)-block-poly(ϵ-caprolactone) copolymer as a carrier for paclitaxel. *J. Controlled Release* **2003**, *89*, 437−446.

(46) Francis, M. F.; Dhara, G.; Winnik, F. M.; Leroux, J.-C. In vitro evaluation of pH-sensitive polymer/niosome complexes. *Biomacromolecules* **2001**, *2*, 741−749.

(47) Heydenreich, A. V.; Westmeier, R.; Pedersen, N.; Poulsen, H. S.; Kristensen, H. G. Preparation and purification of cationic solid lipid nanospheres—effects on particle size, physical stability and cell toxicity. *Int. J. Pharm*. **2003**, *254*, 83−87.

(48) Shelley, J. C.; Shelley, M. Y.; Reeder, R. C.; Bandyopadhyay, S.; Klein, M. L. A coarse grain model for phospholipid simulations. *J. Phys. Chem. B* **2001**, *105*, 4464−4470.

(49) Marrink, S. J.; Mark, A. E. Molecular dynamics simulation of the formation, structure, and dynamics of small phospholipid vesicles. *J. Am. Chem. Soc*. **2003**, *125*, 15233−15242.

(50) Srinivas, G.; Discher, D. E.; Klein, M. L. Self-assembly and properties of diblock copolymers by coarse-grain molecular dynamics. *Nat. Mater*. **2004**, *3*, 589−591.

(51) Moghimi, S. M.; Hunter, A. C.; Murray, J. C.; Szewczyk, A. Cellular distribution of nonionic micelles. *Science* **2004**, *303*, 626−628.

(52) Bermudez, H.; Brannan, A. K.; Hammer, D. A.; Bates, F. S.; Discher, D. E. Molecular weight dependence of polymersome membrane structure, elasticity, and stability. *Macromolecules* **2002**, *35*, 8203−8208.

column (methanol solvent), with retention times of 1.45 min (free dye) and 2.89 min (dye−polymer conjugate). Peak analysis indicates polymer labeling efficiencies of 44% and less than 5% free dye after extensive dialysis.

pH-Dependent Stability of Polymersomes. PEG-PLA or PEG-PCL blended with inert copolymers (e.g., PEG-PBD (PEG-polybutadiene)) provides broad control over release kinetics, with hydrolytically triggered poration proving first-order and dependent on degradation from hours to weeks.[13] Degradable polymersomes here are composed of 25/75 mol % OL2/OB18. These plus inert vesicles of OB18 are prepared by hydration in various aqueous buffers.[13] Stability of giant vesicles is evaluated as a function of pH (5.5 and 7.4) and temperature (4 °C and 37 °C) in closed chambers of isotonic PBS and HEPES buffers. Nanosized vesicles are obtained by sonication, freeze−thaw, and extrusion through 0.4, 0.2, and 0.1-μm polycarbonate filters.[14]

Preparation of Drug-Loaded Polymersomes. Loading of TAX is done after vesicle formation. TAX (in MeOH) is injected in the vesicle suspension with excess drug removed by extensive dialysis. Drug-loading efficiencies are determined by HPLC after drying and redissolving in MeOH. This polymer−drug solution is injected into a C18 column with MeOH as the mobile phase and detection of absorbance at 220 nm.

DOX is loaded into polymersomes by a pH-gradient method developed for liposomes.[53] By hydrating vesicles in citrate buffer (300 mOsm, pH 4.0), a pH gradient is created across the vesicle membrane upon dialysis into pH 7.4 PBS buffer (4 °C). Adding weakly basic DOX allows for its permeation, protonation, and entrapment, with unencapsulated DOX removed by dialysis (MWCO 1 MDa) at 4 °C. Encapsulation efficiency is determined using fluorescence and HPLC (Supplementary Figure 1, Supporting Information) and for polymersomes exceeds 60% of added drug, with drug/copolymer ratios of approximately 1−2 molecules of drug per copolymer. Dual (DOX + TAX)-loaded polymersomes are prepared by sequential loading. Efficiency of TAX loading is measured prior to DOX loading and rechecked independently of excess DOX. All vesicle formulations are sized down by sonication, freeze−thaw cycles, and extrusion as above[14] for subsequent in vitro and in vivo studies.

Cryogenic Transmission Electron Microscopy (Cryo-TEM). Details of cryo-TEM imaging of nanopolymersomes are found in ref 12.

In Vivo Antitumor Activity in Human Breast Carcinoma Xenograft Model. Tumors have been established in nude mice by a single subcutaneous injection of 2×10^6 MDA-MB231 cells with 4 mice total/group. Tumors are allowed to grow to a mean tumor size of $\sim$0.5 cm^2. A single tail-vein injection is done at a maximum tolerated dose (MTD) determined beforehand (as body weight loss <5%) of (DOX + TAX)-loaded polymersomes (DOX at 3 mg/kg; and TAX at 7.5 mg/kg; 0.1 mL injected of 10 mg/mL copolymer equates to 0.5 mg/mL with blood dilution and 37.5 mg/kg). Control groups receive intravenous doses of either empty vesicles, saline, or free drugs at their combined maximum MTD (DOX at 1.5 mg/kg; and TAX at 1.0 mg/kg). Combination therapy is preferred over individual drug treatments because of the synergistic potency of dual drug formulations observed in initial MTD measurements. MTD of combination (DOX + TAX)-loaded polymersomes (DOX at 2.5 mg/kg; and TAX at 2.5 mg/kg) is less than that of DOX-polymersomes (>10 mg/kg) and TAX-loaded polymersomes (7.5 mg/kg). Tumor size (±SEM) is measured in two orthogonal dimensions [$(L_1 \times L_2)/2$] at 1−7 days for each treatment group, and tumor size data for (DOX + TAX)-loaded polymersomes is normalized to the tumor size of saline and empty vesicle control groups. Apoptosis in tumor tissue, 48 h post polymersome−drug injection, is detected by Tdt-mediated dUTP nick-end labeling (TUNEL) using a commercial kit according to the manufacturer's instructions as previously described.[54]

Cell Culture, Internalization, and Cytotoxicity. Human breast cancer epithelial cells, MDA-MB231, are grown in glucose-rich, pyruvate-free DMEM (Life Technologies, Inc.), and human lung carcinoma cells A549 (ATCC) in F12 Ham media. Both cultures are supplemented with 10% fetal bovine serum (BM), 2 mM glutamine, 100 units of penicillin, and 100 μg of streptomycin and maintained at 37 °C in 5% CO_2 and 95% humidified air. Cells were plated in 24-well plates (10^5 cells/mL) and cultured for 24 h before polymersome addition.

Cell uptake of empty nanopolymersomes is determined by incubating fluorescently tagged vesicles with MDA cells. For tracking vesicles, 5 mol % of OB18 copolymer is covalently labeled with fluorophore and blended into the vesicles. For temperature studies, cells are preincubated at the designated temperatures for 1 h prior to addition of polymer vesicles. Inhibitors of vesicle uptake include sucrose (450 mM), nocodazole (10 μg/mL), genistein (200 μM), and chlorpromazine (10 μg/mL) with preincubations for 1 h, at 37 °C. Following addition of fluorescently labeled vesicles, cells are washed with serum-free media and visualized in fluorescence (60×, 1.4 numerical aperture).

The two cancer cell lines are exposed to free drugs or nanopolymersome formulations of various dilution for 3 or 12 h, washed with media, and then incubated drug-free either for toxicity kinetics or, after 24 h, for dose−response. Cytotoxicity is assayed colorimetrically: MTT reagent (in PBS) is added to 0.5 mg/mL, and a 3 h incubation at 37 °C allows viable cells to reduce the yellow MTT solution to blue Formosan crystals that are soluble in detergent. Absorbance at 550 nm of wells was measured with a microplate reader (Molecular Devices; Palo Alto, CA).

(53) Mayer, L. D.; Bally, M. B.; Cullis, P. R. Uptake of adriamycin into large unilamellar vesicles in response to a pH gradient. *Biochim. Biophys. Acta* **1986**, *857*, 123−126.

(54) Persad, R.; Liu, C.; Wu, T.-T.; Houlihan, P. S.; Hamilton, S. R.; Diehl, A. M.; Rashid, A. Overexpression of caspase-3 in hepatocellular carcinomas. *Mod. Pathol*. **2004**, *17*, 861−867.

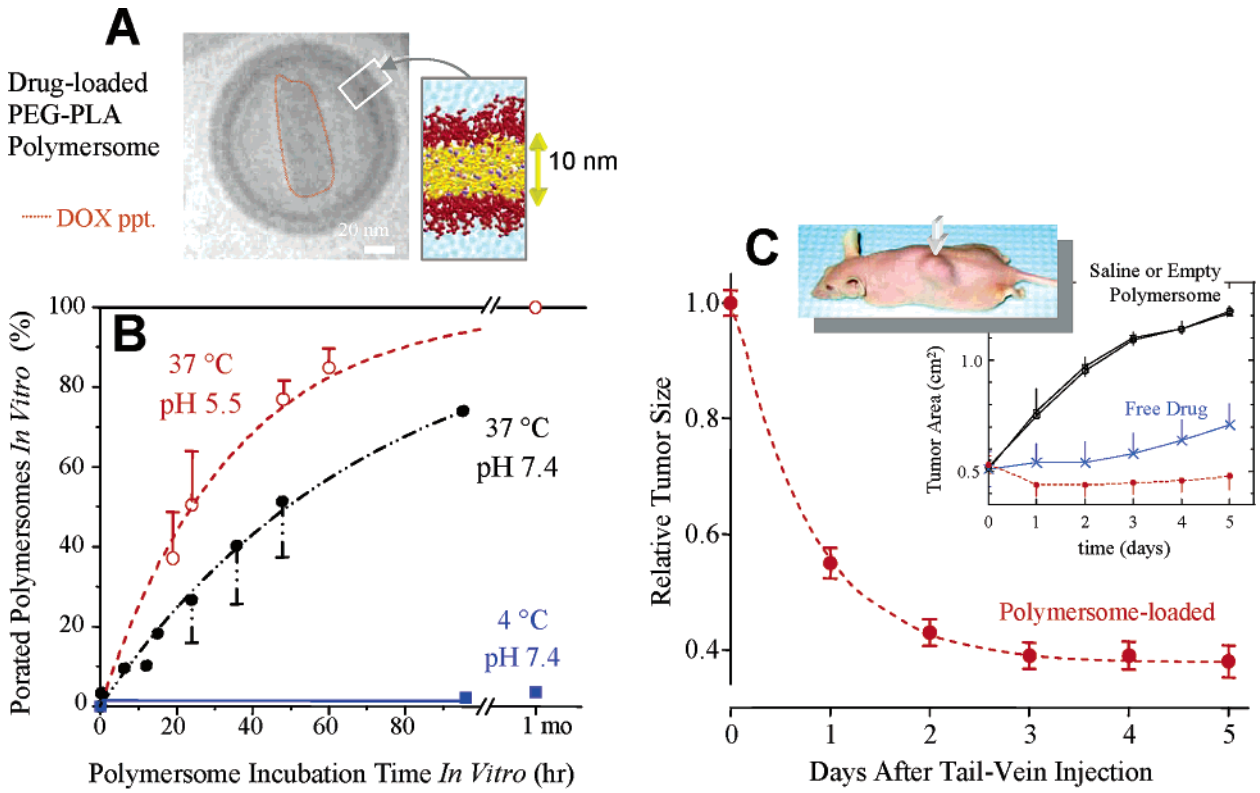

Figure 1. Drug loading, release, and antitumor activity of degradable polymersomes. (A) Cryo-TEM image of DOX- and TAX-loaded nanopolymersome. DOX permeates and precipitates as an aggregate (ppt., circumscribed) within the PEG-PLA-based vesicles, whereas TAX intercalates into the ~10 nm thick hydrophobic core visible with fluorescent-TAX (Supplementary Figure 1). (B) Degradable giant vesicles visibly porate and release encapsulants in isotonic PBS, pH 7.4 at 37 °C and even faster in isotonic HEPES, pH 5.5 at 37 °C ($\tau_{pH5.5} = 0.49\tau_{pH7.4}$); but the vesicles are stable in PBS at 4 °C. (C) Solid tumors shrink after a single injection of (DOX + TAX)-loaded polymersomes. Tumors are obtained by implanting human breast cancer derived cells (MDA-MB231; 2×10^6 cells) subcutaneously in nude mice, and then allowing the resulting nodule to grow to a diameter of about 0.5 cm^2 (arrow). For treatment, either drug-loaded polymersomes (red), free drug (blue), or empty polymersome or saline control was injected in the tail vein (4 mice per group). Tumors in both control groups double in size within 2 days, whereas the tumor area (mean ± SD) with drug-loaded polymersomes shrinks. The relative tumor area accounts for growth suppression plus shrinkage and is fit with a two-step model in the text that parallels in vitro studies of polymersomes.

Results and Discussion

Drug-Loaded, Degradable Polymersomes. Partitioning of insoluble TAX into the polymersome membranes appears almost 10-fold more efficient (per mass) than reported for liposomes.[18] The difference is most likely due to the much thicker membranes of polymersomes (Figure 1A) compared to liposomes (with ~3 nm thick cores). DOX is also readily loaded into polymersomes using a pH-gradient method in which neutral DOX (DOX^0) permeates the polymersome and coprecipitates as charged DOX^+ with citrate in the lumen, leading to fibrous aggregates visible in cryo-TEM (Figure 1A), as seen previously with liposomes.[26] Fluorescence imaging of DOX within giant vesicles together with HPLC analysis (Supplementary Figure 1) establishes loading efficiencies similar to those of liposomes.[27]

Polyester hydrolysis is widely exploited for biocompatible applications[28] and is well-known to be accelerated by acidic pH,[29] but polyester-based copolymer vesicles are new to exploit the phase behavior of block copolymer amphiphiles. PEG-PLA-based vesicles show that hydrolysis of the PLA is indeed accelerated with mild acidity, but temperature shifts can have a greater effect. At pH 5.5 and 37 °C, conditions relevant to endolysosomes, the majority of vesicles are porated within 1−2 days (Figure 1B), with chain degradation confirmed by HPLC (Supplementary Figure 2, Supporting Information). Time constants nearly double in neutral buffer (Figure 1B). At 4 °C, however, leakage from both vesicles is minimal, with <5% of encapsulant lost after 1 month, which is convenient for storage of vesicles. We estimate from such temperature studies an activation energy for hydrolysis (at pH 7) of about 40 kJ/mol, which compares well with hydrolysis of aqueous polyesters.

Shrinking Tumors with (DOX + TAX)-Polymersomes. Solid tumors in nude mice were obtained by subcutaneous injection of MDA-MB231 human breast cancer cells. These cells are known for yielding highly invasive, hormone-independent models of breast tumors.[30] Such tumors are also known to have a leaky vasculature that allows permeation of nontargeted carriers by the well-known enhanced permeation and retention (EPR) effect.[31]

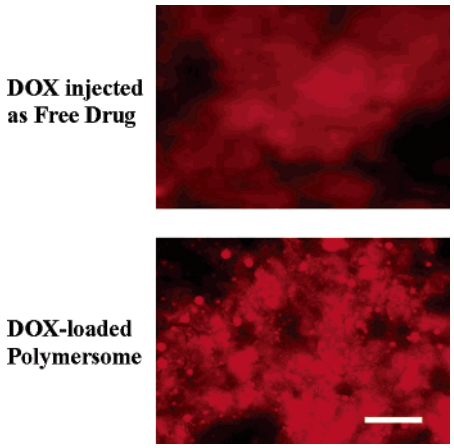

Figure 2. Fluorescent detection of free DOX and polymersome-encapsulated DOX in tumor sections. Sections were made 5 μm thick; scalebar is 20 μm. Large increases in fluorescent punctates (>100 vesicle spots per section) were observed in tumors 24 h after polymersome−drug treatment.

On the day of treatment, tumors in all control and treatment groups were approximately the same size (Figure 1C, upper inset). Single injections of either (TAX + DOX)-polymersomes or free drugs at their maximally tolerated dose (MTD) or else controls (systemic injection of buffer or empty polymersomes) were then followed by daily monitoring of tumor sizes relative to controls. Whereas the control tumors continued to grow and double in size within about 2 days, the polymersome treatments shrank these rapidly growing tumors, which showed no significant increase in tumor size out to 5 days. Tumors treated with free drugs did not shrink and had instead grown 50% by 5 days. Drug-loaded polymersomes thus blocked tumor growth or cell proliferation (expected of TAX) and also killed cells (expected of DOX and TAX). We plot in Figure 1C the relative tumor size after polymersome injection in order to compare the in vivo kinetics to in vitro kinetics.

DOX fluorescence allows for direct visualization of drug accumulation in the tumor and shows, 24 h after injection, punctate fluorescence for drug-loaded polymersomes but only diffuse fluorescence for free drug (Figure 2). The polymersomes evidently release their drug because they also cause massive tumor cell apoptosis within 48 h of treatment, as assessed by TUNEL staining (data not shown).

The in vivo results suggest that systemic injection of polymersomes leads first to vesicle localization, with time constant τ_{uptake}, and subsequent cytotoxicity, τ_{toxic}. Past analyses of systemic delivery to tumors by stealth liposomes using the EPR effect have also exploited relatively simple two-time-constant models.[25] We fit our in vivo tumor shrinkage results (Figure 1C) with a simple two-step, X → Y → Z pharmacokinetic model:

$$\text{tumor size} = 1.0 - \{A[(1/\tau_1) - (1/\tau_2)]^{-1}\}[1 - (1/\tau_2) \exp(-t/\tau_1) + (1/\tau_1)\exp(-t/\tau_2)] \quad (1)$$

Our fit yields $\tau_1 = \tau_{\text{uptake}} = 1$ h for localization after systemic delivery and $\tau_2 = \tau_{\text{toxic}} = 16-18$ h for subsequent cytotoxicity. Below we relate these time constants to cellular pathways of polymersome-based delivery in vitro—from vesicle entry and endolysosomal rupture to cytotoxic effects—paying particular attention to a similarity in kinetics. Table 2 summarizes the fit above and those that follow below.

Table 2. Polymersome Kinetics in Vivo and in Vitro

process	time constant (h)	figure	eq
in vivo			
tumor uptake of polymersome	1	1C	1
cytotoxicity and growth inhibition	16−18	1C	1
in vitro			
cell uptake of polymersome	1−2	5	2
polymersome cytotoxicity in cell culture	10−12	4B	
polymersome-induced membrane lysis	12	6B	
endolysosomal escape	12−14	5	2
drug release in dialysis (pH 5.5)	17−19	4A	

In Vitro Uptake and pH-Enhanced Release from Degradable Polymersomes. To first clarify vesicle entry, fluorescently labeled polymersomes were added to cultures of breast cancer cells using polymersome concentrations similar to those in vivo. Subsequent imaging (shown herein) indicates that vesicle uptake saturates within hour(s), which is consistent with internalization of PLGA nanoparticles.[32] Vesicles initially appear punctate throughout a cell, but by 10 h they appear to have accumulated in the perinuclear region (Figure 3A). Savic and co-workers[8] have shown that PEG-PCL copolymer micelles will also enter cells and redistribute.

The PEG-ylated polymersomes here lack any specific targeting moieties and are also "stealthy" (showing minimal phagocytosis) for many hours,[14,33] which tentatively suggests that polymersome uptake occurs in proportion to local concentration via fluid phase pinocytosis. Such entry still has active features and can couple to other internalization pathways. Indeed, incubation at 4 °C (for 4 h) reduces polymersome pinocytosis by almost 90% compared to 37 °C. Similar temperature-dependent reductions in uptake (~80%) have also been seen with PLGA nanoparticles,[32] pointing to energy dependent processes of internalization. Further treatments show mixed effects. Polymersome uptake is not affected by microtubule disruption with nocodazole, which is known to limit intracellular trafficking and may affect perinuclear localization.[34] In contrast, polymersome uptake decreases to ~30% of controls in a hypertonic culture medium achieved by adding sucrose, which tends to shrink cells and inhibit endocytosis.[32] Such results appear consistent with recent reports for 200 nm beads[35] as well as PLGA particle uptake via pinocytosis.[32] Inhibiting clathrin-mediated endocytosis (with chlorpromazine) and caveolae-mediated endocytosis (with genistein) also reduces polymersome internalization (to 38% and ~20%, respectively), which is similar to results for inhibited uptake of 50 nm beads.[35] Select energy-dependent import pathways thus appear coupled in what tentatively appears to be pinocytotic uptake of the nontargeted polymersomes here.

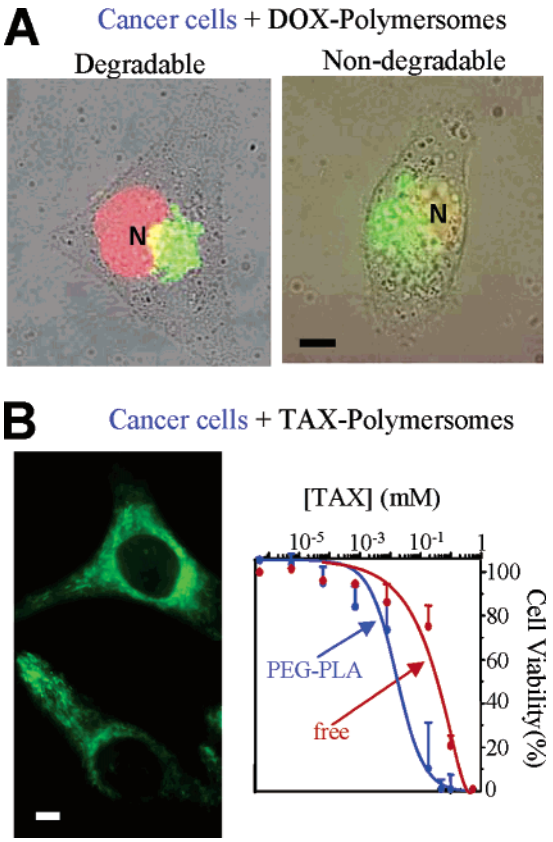

Figure 3. Intracellular delivery and toxicity in cell culture of DOX- and TAX-loaded polymersomes. (A) Overlap of bright field and fluorescence images of DOX (red) delivered by polymersomes (green-labeled copolymer) that are either degradable or nondegradable. Cells were exposed to DOX-polymersomes (15 μg/mL DOX in 0.5 mg/mL copolymer) for 3 h (saturated uptake), then washed, and imaged over 24 h. Scale bar is 5 μm. (B) In vitro delivery and dose−response of TAX-loaded polymersomes versus free drug. TIRF-imaged cellular internalization of fluorescent-TAX polymersomes. After 24 h, cell proliferation was determined by MTT assay and cell death fit with standard dose−response curves of the form $y = (100\%)K^p/(K^p + x^p)$. Empty polymersomes have no effect on viability.

Cellular Localization and pH-Enhanced Release from Degradable Polymersomes. Drug delivery and release within breast cancer cells by polymersomes has been directly imaged by two-color fluorescence microscopy (Figure 3A): DOX fluoresces red while labeled vesicles fluoresce green. Overlap gives yellow and indicates intact polymersomes. Only degradable vesicles show any distinct color separation at times less than 12 h: DOX intercalates into DNA[36] and causes nuclei to fluoresce red while green-labeled copolymer remains perinuclear. TAX is also released from degradable polymersomes on similar time scales, and it stains, when fluorescent, linear structures likely to be microtubules (Figure 3B). With inert vesicles, DOX will leak and provide similar pictures, but on much longer time scales (by 48 h).

Microdialysis studies done in acidic buffer show that both DOX and TAX are released from degradable polymersomes (Figure 4A) with time constants of $\tau_{release} \cong 18$ h, which is remarkably similar to tumor shrinkage times (Figure 1C; Table 2). In neutral pH buffer, dialysis gives considerably longer time constants. In addition, leakage from the non-degradable vesicles (of OB18) is severalfold slower.

In contrast to polymersome-based delivery, DOX^0 added as a free drug to cell culture diffuses across cell membranes (leading to cardiotoxicity in organisms) and permeates far more rapidly than across polymersome membranes (on the basis of loading times). Upon permeation of free drug, DOX fluorescence fills the entire cytoplasm and nucleus, and after many hours, membrane blebs emerge, indicative of necrosis that is not seen with polymersome delivery. DOX delivery with conventional liposomes can be more ambiguous and sometimes causes only a delay in proliferation.[37]

The results above suggest that internalization of polymersomes followed by centripetal transport to the nucleus[38] fosters drug binding to DNA in ways distinct from other delivery methods. Cytotoxicity results for both DOX and TAX confirm the effectiveness of degradable polymersomes in cell culture and prove remarkably consistent with in vivo time scales (Figure 1C). Indeed, after addition of degradable DOX-loaded polymersomes, MTT assays yield a time constant of 12 h (Figure 4B), which is in good agreement with all of the results above. Inert polymersomes, in spite of similar cell-entry kinetics, are again severalfold slower in their cytotoxic effects (48 h) (Figure 4B). Additionally, free TAX, like DOX, permeates and kills cells, but the IC_{50} for free TAX is nearly 40-fold above the 6 μg/mL found for the degradable polymersomes (Figure 3B). We propose that the same type of endolysosomal escape seen with DOX from degradable polymersomes enhances the toxicity of TAX; indeed, paclitaxel delivery from nondegradable vesicles is less effective (4−5-fold slower) than with degradable polymersomes. Parallel studies with breast cancer cells and lung carcinoma cells (A549) show similar dose response curves and cytotoxicity time constants (10 and 18 h, respectively; Figure 4C).

Carriers often reduce IC_{50}s through improved drug solubility, more efficient uptake (endocytic entry versus drug permeation), and—upon release—improved trafficking within the cell.[39−41] The various kinetic measures above imply that, with inert polymersomes, passive leakage of DOX or TAX is minimally dependent on the low pH of the endolysosome,[42−44] whereas endolysosomal acidity accelerates hydrolytic scission of degradable PLA chains and triggers endolysosomal rupture. The molecular mechanism that is exploited is elucidated below.

Mechanism of Degradable Polymersome-Mediated Drug Delivery. Using the endosome selective dye Lysotracker Blue, fluorescence microscopy of breast cancer cells shows progressive colocalization of red-labeled, degradable vesicles as pink in a blue + red color overlay (Figure 5). Initially, cell-localized vesicles appear red and are seen at the cell periphery, but some colocalization is clear by 1−2 h; nondegradable vesicles (Figure 5, upper left inset) indeed show that uptake occurs with a time constant of 1−2 h

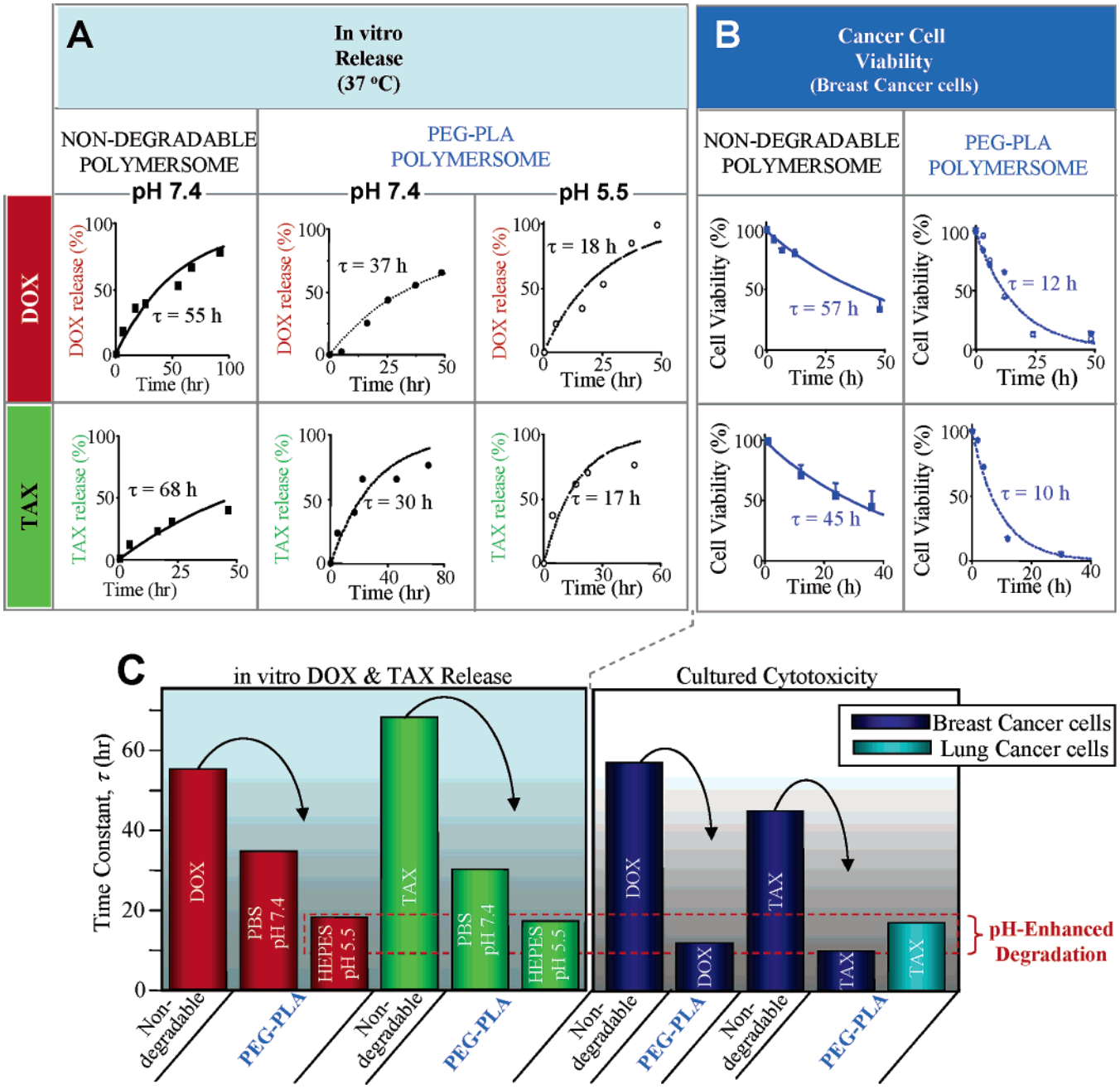

Figure 4. Kinetics of in vitro release and cytotoxicity of DOX- and TAX-loaded polymersomes. (A) In vitro release and leakage of drugs (DOX and TAX) from degradable and nondegradable polymersomes into PBS (pH 7.4) and either HEPES or MES-saline (pH 5.5) at 37 °C. DOX release into bulk during dialysis is monitored by fluorescence (Ex 470 nm, Em 586 nm), and TAX release into buffer during dialysis is measured by reverse phase HPLC (at 220 nm) on polymer−drug aliquots dissolved in 100% methanol. Free drug releases into bulk within <3 h, indicating that the dialysis membrane does not hinder drug release. (B) Cytotoxicity kinetics of degradable versus nondegradable DOX- and TAX-loaded polymersomes (at 35 μg/mL) as determined by MTT assay. Fits are first order to obtain the toxicity time τ_{toxic}. Data was compiled from two to four independent MTT experiments each done in triplicate (mean ± SEM). (C) Summary of in vitro DOX and TAX release ($\tau_{release}$) and cytotoxicity (τ_{toxic}) kinetics for both MDA breast cancer cells and A549 lung cancer cells. The highlighted range for pH-enhanced degradation is about 10−20 h across all of the measurements.

without complications of copolymer degradation. Pretreatment of cells with ammonium chloride, which raises endosomal pH and can also lyse endosomes, diminishes polymersome uptake and colocalization at the 4 h peak by more than half. At later times (12 h), sufficient for copolymer hydrolysis, polymersome fluorescence is a diffuse red. This suggests not only that a substantial fraction of labeled vesicles have escaped endolysosomes and dispersed within the cytosol

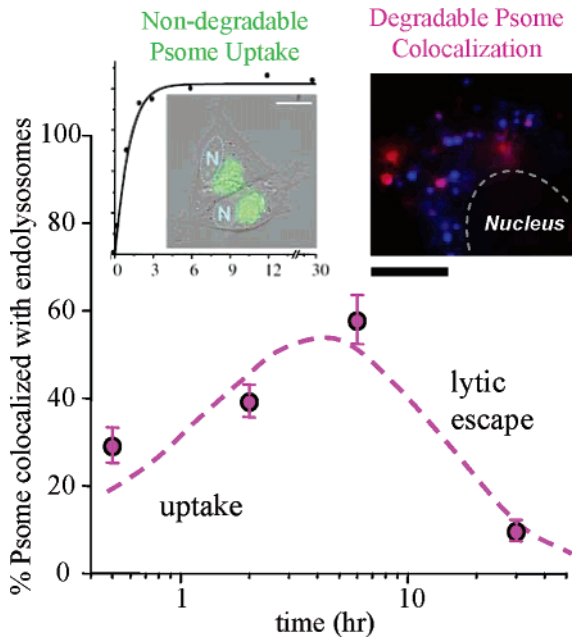

Figure 5. Intracellular tracking of degradable polymersomes and endolysosomes. Vesicles were prelabeled with the hydrophobic dye (red) for colocalization with the endosomes (blue), as shown in the upper right inset. Breast cancer cells were incubated with polymersomes for 3 h, washed, and then incubated for the indicated times before staining with the endosomal marker Lysotracker Blue (50 nM; 30 min). Scale bar is 10 μm. The upper left inset shows the control experiment for uptake of green-labeled, inert polymersomes. The dashed curve fit is eq 2 in text.

but also that vesicles are degrading. At later times of 1−2 days, new endolysosomes appear blue and seem unaffected by past exposure to copolymer.

The results above indicate a transient and nontoxic interaction between copolymer and endolysosomal membranes. A simple uptake−escape model that fits the data of Figure 5 is provided by the same two-step, X → Y → Z kinetic model for eq 1, but here we follow the accumulation and decay of the intermediate Y:

$$\text{colocalization} = B[1 - (\tau_1/\tau_2)]^{-1}[\exp(-t/\tau_2) - \exp(-t/\tau_1)] \quad (2)$$

The fit yields $\tau_1 = \tau_{\text{uptake}} = 2$ h, which is consistent with the internalization results for nondegradable vesicles (Figure 5, left inset). The fit also gives $\tau_2 = \tau_{\text{escape}} = 14$ h, which reinforces the finding that cytotoxicity has a shorter time scale than acid-induced release; see Table 2. This suggests that either the initial drug release or the endolysosomal rupture itself is especially cytotoxic.

Physical interactions between the various diblock copolymers and cell membranes were directly examined by incubating a wide range of copolymer concentrations (0−200 mg/mL) with red blood cells (RBCs). RBCs are certainly relevant to any possible hemolysis upon intravenous injection (Figure 1C); but RBCs also approximate endolysosomal membranes with a typical mixture of phospholipids, cholesterol, and integral membrane proteins. After copolymer incubations of 24 h at 37 °C, intact cells and bulk polymer were removed by centrifugation, and hemoglobin in the supernatant was monitored. The PEG-PLA copolymer, OL2, caused hemolysis of RBCs at a critical poration concentration (C_{CPC}) of 75 mg/mL copolymer (Figure 6A). In comparison, the inert block copolymer, OB18, did not disrupt cell membranes up to 200 mg/mL. Because OL2 is nearly symmetric ($f_{\text{EO}} \approx 0.5$) before any PLA hydrolysis, its tendency to form micelles increases with even the slightest degradation,[6,13] making it increasingly surfactant-like. Further RBC incubation with fluorescently tagged and purified TMRCA-OL2 shows lysed, red-fluorescent RBCs as a few bright spots (Figure 6A, inset). Kinetic studies at 100 mg/mL copolymer ($> C_{\text{CPC}}$ of OL2) demonstrate exponentially increasing lysis by OL2 with a time constant of 12 h (Figure 6B), and a twice-longer time constant for a PEG-PCL copolymer that is initially more of a membrane former than a micelle former ($f_{\text{EO}} < 0.5$). In comparison, the small surfactant Triton X-100 ($f \cong 0.7$) at ~1 mM lyses 100% of red cells within hours. The degradable copolymers here are thus time-evolving detergents with an increasing potential for membrane-disruptive surfactant activity at high copolymer concentrations ($> C_{\text{CPC}}$). Because critical aggregation concentrations are proportional to aggregation kinetics[6] and because scaling in solubilization across detergent, lipid, and copolymer amphiphile systems has already been established,[55] the lysis results here suggest

$$C_{\text{CPC}} \sim f^{-\alpha} M_{\text{h}}^{\beta}$$

with tentative scaling exponents of $\alpha = 0.3$ and $\beta = 1.5$. Such a relationship implies that membrane-preferring copolymers (low f) or high molecular weight copolymers are slow to interact with lipid membranes such as endolysosomes.

While similar hemolytic tests by Jeong et al.[45] with degradable micelles of poly(2-ethyl-2-oxazoline)-PCL did not report any lytic activity, the 10 mg/mL copolymer concentrations tested by Jeong et al. are well below the C_{CPC}s here and their incubation times of 30 min appear far too short. Despite the potential membrane-lytic activity of these copolymers, our treatment concentrations up to a few milligrams per milliliter (mg/mL) both in vivo and in vitro are well below the C_{CPC}. Empty polymersomes up to 2 mg/mL copolymer indeed show no cytotoxic effects on the breast cancer cells in standard MTT assays. Liposomal systems are similarly nontoxic at low concentration,[46] but some systems that use surfactants in preparation such as polymer/niosome complexes[46] and solid nanospheres[47] can be cytotoxic at such concentrations.

The results above for the copolymer C_{CPC} are nonetheless critically important to understand the pathway of drugs

(55) Pata, V.; Ahmed, F.; Discher, D. E..; Dan, N. Membrane solubilization by detergent: resistance conferred by thickness. *Langmuir* **2004**, *20*, 3888−3893.

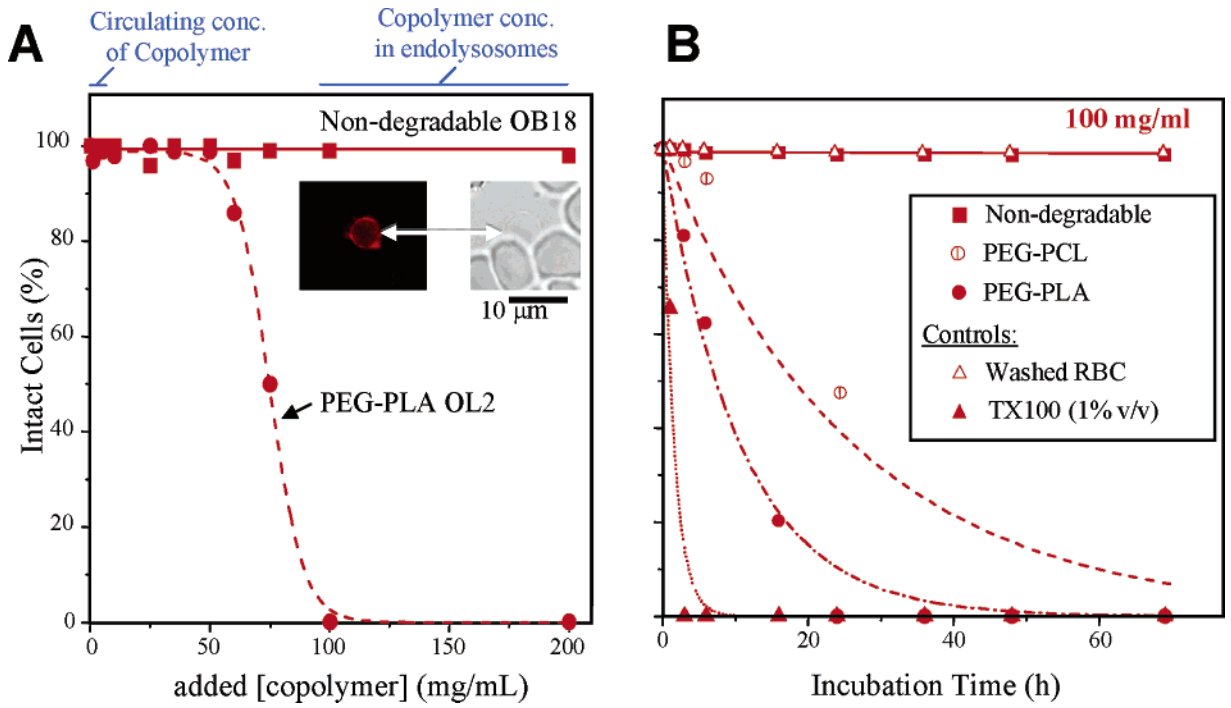

Figure 6. Concentration dependence and kinetics of cell membrane rupture by block copolymers. (A) Hemolysis of RBCs (at 5% hematocrit in PBS) occurs with degradable PEG-PLA (OL2) after 24 h at 37 °C but not with nondegradable copolymer (OB18). The copolymer concentration at 50% lysis defines a C_{CPC} of 75 mg/mL for OL2. Inset shows fluorescent OL2 integrates into the membranes of hemolyzed RBCs. (B) Polymer-mediated RBC lysis displays standard, first-order kinetics. Block copolymer films of degradable OL2 or nondegradable OB18 were hydrated (to 100 mg/mL) with washed RBCs (at 5% hematocrit) for 24 h at 37 °C. Postincubation the samples were centrifuged and the supernatant assayed for hemolysis (absorbance at 540 nm).

delivered by polymersomes. Circulating concentrations of copolymer are low (Figure 6A), but once internalized, the local concentration of surfactant-like copolymer increases dramatically: a 400 nm endolysosomal vesicle with a single 100 nm polymersome within it yields a copolymer concentration of about 125 mg/mL. This is well above the C_{CPC} (see Figure 6A) and is more than sufficient to rupture an endosome.

The concentrating effect being described is a direct result of the discrete or quantal nature of endocytosis and trafficking in cells; the nerve synapse provides perhaps the classic example of such quantal, burst-release type of trafficking. Degradable polymersomes thus foster delivery of drugs to their targets within cells by generating copolymer macrosurfactants that destabilize both the vesicle and the endolysosome.

Molecular Simulations of Interactions. Does the C_{CPC} reflect interactions of membranes, micelles, or unimers of copolymer with cell membranes? Addressing such questions of carrier interactions with cell systems by molecular simulation can be challenging for computation. However, rational methods of coarse graining the atomistic interactions have recently reproduced not only the self-assembly of large patches of phospholipid membranes[48,49] but also the membrane-through-micelle phase behavior of PEG-based copolymers used here.[50] Increasing the copolymer hydrophilic fraction, f_{EO}, by a mere 10% is sufficient to transform a membrane-forming block copolymer in water into a micelle former. The copolymers simulated here self-assemble into membranes and micelles (listed in Supplementary Table 1, Supporting Information) and effectively represent a range of PEG-polyester chains shortened by hydrolysis as occurs in experiment.

Copolymers with small f_{EO} that self-assemble into continuous bilayer structures appear inert and devoid of any significant interactions with an adjacent lipid bilayer (Figure 7). Copolymers with higher f_{EO} self-assemble into micellar morphologies, and, in time, spherical micelles interact strongly with the lipid bilayers. PEG arms extend toward the lipids as the polar lipid headgroups provide a favorable environment for transient PEG insertion. Note that although PEG is generally considered hydrophilic, it is known to exhibit surfactant-like activity in partitioning to an air−water interface at micromole per liter concentrations (μM) for M_{EO} ~ 1000 kDa ($C_{partn} \sim M_{EO}^{-1.9}$ from fits of data in Zeno et al.[56]) and it also binds the headgroups of surfactants, stabilizing micelles.[57] The weak tethering that develops here

(56) Zeno, E.; Beneventi, D.; Carre, B. Interactions between poly-(ethylene oxide) and fatty acids sodium salts studied by surface tension measurements. *J. Colloid Interface Sci.* **2004**, *277* (1), 215−220.

(57) Zanette, D.; Soldi, V.; Romani, A. P.; Gehlen, M. H. The Role of the Carboxylate Head Group in the Interaction of Sodium Dodecanoate with Poly(ethylene oxide) Investigated by Electrical Conductivity, Viscosity, and Aggregation Number Measurements. *J. Colloid Interface Sci*. **2002**, *246* (2), 387−392.

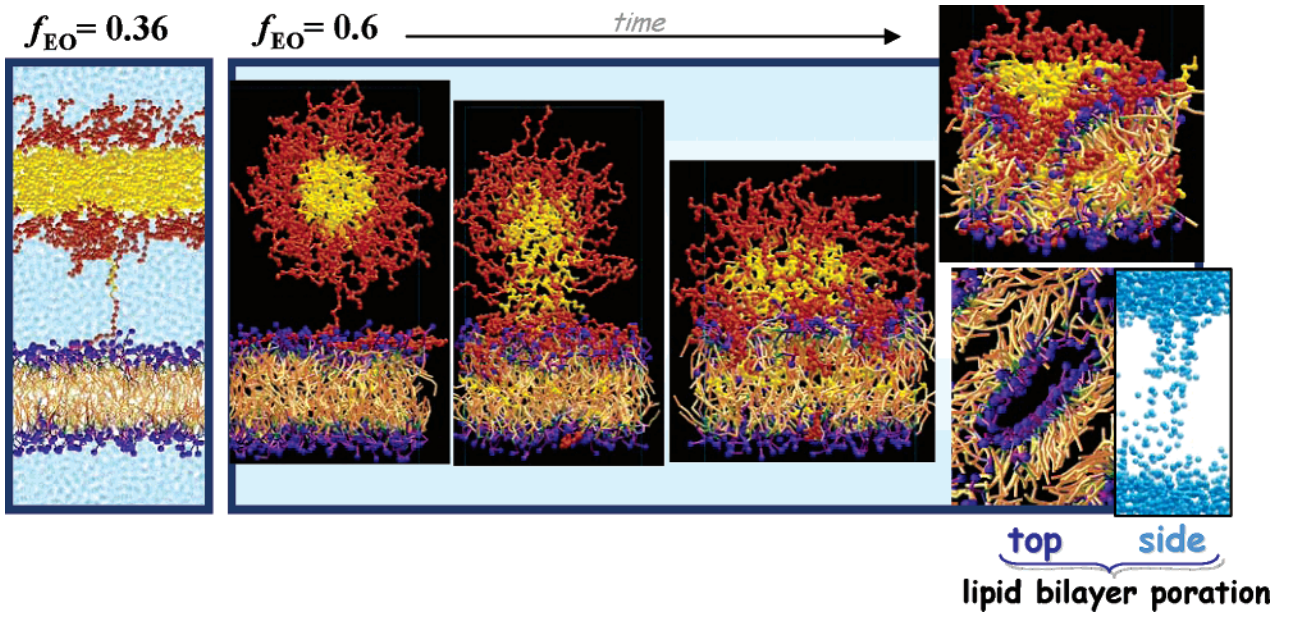

Figure 7. Molecular dynamics of block copolymer interactions with lipid membranes. Hydrophilic and hydrophobic blocks of copolymer are represented as red and yellow spheres, while the lipid heads are violet and the tails are pale yellow. Water is light blue. Copolymers with $f_{EO} = 0.36$ form stable bilayers and do not interact with lipid bilayers. Copolymers having larger f_{EO} self-assemble into micelles, which can interact with a lipid bilayer over time. Pore formation due to copolymer insertion into lipid bilayer is shown in top view (at 7.5 ns) without the copolymers and, in side view, just for water.

in simulation is followed by copolymer transfer of the hydrophobic tails from the micelle into the lipid membrane, which increases until the whole micelle integrates and mixes into the lipid membrane. Just as one expects with small detergents, curvature imparted by the micelle leads to pores in the membrane through which water—and soluble drug—will diffuse. PEG appears to prop open these pores and facilitate permeation (Supplementary Figure 3, Supporting Information).

The simulations fit our experiments and may help clarify a controversial mechanism of drug delivery reported recently with micelles of PEG-PCL.[8,51] Our simulations show that while self-assembled membranes of copolymer and self-assembled membranes of lipid interact very little, very similar copolymers assembled into spherical micelles will fuse, mix, and porate a lipid membrane. If the micelles are generated by polymersome degradation, the same process applies. Given that the membrane of an endolysosome is the cell's last barrier to cytoplasmic entry, the copolymer-mediated poration seen here clearly creates a new pathway for drug escape and delivery to cellular targets.

Acknowledgment. We thank Prof. Valerie Weaver for the MDA-MB231 cells. We also thank Silvia Muro Galindo, Penney Gilbert, Younghoon Kim, Robert Bucki, Peter Photos, Shamik Sen, and Nishant Bhasin for technical insight and fruitful discussions. Support for this work was provided by an NIH-R21 grant (D.E.D.), an NSF-PECASE grant (D.E.D.), an NSF-MRSEC grant for computational support (M.L.K.), and the Nanotechnnology Institute, NTI (D.E.D.).

Supporting Information Available: Figures depicting DOX and TAX loading capabilities of polymersomes, degradation kinetics of PEG-PLA blended formulations, and spatial correlations between the density of PEG and water molecules in the lipid membrane; table of data from simulations of f_{EO}-dependent copolymer−lipid bilayer interactions; details of materials and methods. This material is available free of charge via the Internet at http://pubs.acs.org.

MP050103U